A Multinodal Model for Surface Contamination Based upon the Boltzmann Equation of Transport

by

E. A. Zeiner
Aerojet ElectroSystems Company

Abstract

A composite analytical model to compute the deposition rates of volatile condensible materials (VCM) on the surfaces of a multinodal enclosure is derived using a Fick diffusion model for the VCM mass loss rates from the source material, an exponential-Langmuir model to account for the reemission rates of deposited VCM, and a Krook relaxation model of the Boltzmann equation to characterize the scattering and transport properties of the VCM between the enclosure nodes.

1. Introduction

The first step in accounting for the influence of filmwise contamination on the sensitive surfaces of a satellite is to determine the amount of contamination deposition on each such receptor surface as time of flight progresses. The second step is to evaluate the thermo-optical effects of these surface deposits. This report describes the properties of an analytical model which has been recently developed to compute the deposition of the volatile condensible materials (VCM) which diffuse out of a nonmetallic source and are eventually deposited on a remote receptor surface.

The overall model (or algorithm) is a composite of these "sub"-models which characterize the basic processes involved in the transfer of the VCM from its host source to the receptor. The first such process is that of source kinetics. This involves the mechanisms by which the VCM moves through the bulk of the host source when the ambient pressure is sufficiently reduced and is eventually released at the source surface. Fick's First and Second Laws for unsteady-state diffusion are employed to model this process. The second process is that of the reemission of the VCM from the receptors on which the adsorbed molecules reside for a short period of time. Based upon experimental evidence[1,2] this process exhibits an exponential reemission rate for very small deposits which becomes a constant rate independent of the deposit thickness[3] where relatively large deposits exist. This latter constant large-mass reemission rate can be identified with the classical Langmuir evaporation mass rate for pure substances, which is a function of the saturation vapor pressure.

The third process is the mass transfer of the VCM molecular streams between the receptor surfaces nodes. This transport model couples the source and reemission kinetics with the relative geometry of the surface nodes which make up the bounding enclosure. The basis for such

a statistical model is the Boltzmann equation for the velocity destribution function (VDF) of the VCM streams. The general intractability of this equation usually requires a simplification of the collision integrals of the Boltzmann equation, which will still permit utilization of the resulting macroscopic flux vectors (velocity moments) for VCM vapor densities varying from continuum viscous flow (Navier-Stokes equations) to collisionless free molecule flow. For this algorithm, the Krook[4] single-relaxation approximation is applied using the "two-stream Maxwellian" distribution of Lees[5]. The initial Maxwellian originates at the enclosure surfaces following source emission, receptor scatter, and receptor reemission as a boundary condition, and then "relaxes" to the uniform Maxwellian of the VCM vapor, which can be approximated as an ideal random gas in local equilibrium with the enclosure surfaces.

The final result is a set of ordinary second-order nonlinear nonhomogeneous differential equations which are coupled together by experimentally determined capture coefficients and the view factors of the nodal surfaces. The collisional properties using the Krook approximation of a symmetric collision frequency parameter restrict this model to gas interactions between similar molecules.

2. Source Kinetics

The release of the VCM from the source material is modeled as a surface-mediated diffusion process. By this is meant that the classical diffusion of VCM molecules through the bulk of the source matrix is influenced by the kinetics of these molecules when they reach the surface of the source and are released. The bulk diffusion process is characterized by a mass diffusion coefficient, while the surface process is characterized by a surface residence time or, its inverse, a rate constant. Both of these parameters are temperature-dependent and must be experimentally determined. A third parameter which must also be empirically

determined is initial quantity of "active" (capable of release from the source) VCM within the source. This obviously specifies the initial uniform concentration.

The governing equation is the one-dimensional form of Fick's Second Law for unsteady state as follows:

$$\frac{\partial C_i}{\partial t} = D_i\left(\frac{\partial^2 C_i}{\partial x^2}\right) \tag{1}$$

where

$C_i(x,t)$ = mass concentration of the i^{th} active component in the source, $g\text{-}cm^{-3}$

D_i = i^{th} component mass diffusion coefficient, $cm^2 - s^{-1}$

x = transverse position in the source coating measured from the free surface, cm

The one-dimensional model is sketched at the left of Figure 1.

The initial concentration of VCM in the source is considered to be uniform so that

$$C_i(o,x) \equiv C_{oi} = \left(\frac{\mu_i W_s}{A_s h}\right) \ g\text{-}cm^{-3} \tag{2}$$

where

C_{oi} = initial mass concentration (density) of the i^{th} active component in the source, $g\text{-}cm^{-3}$

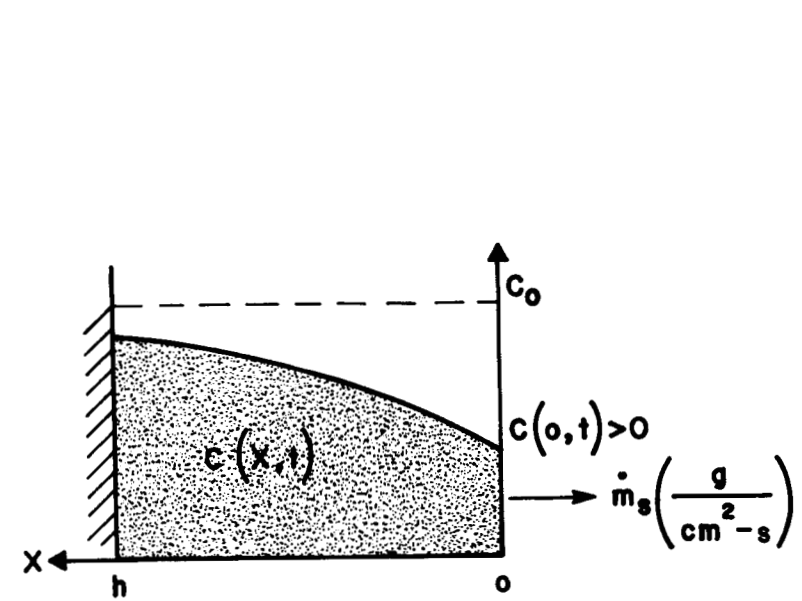

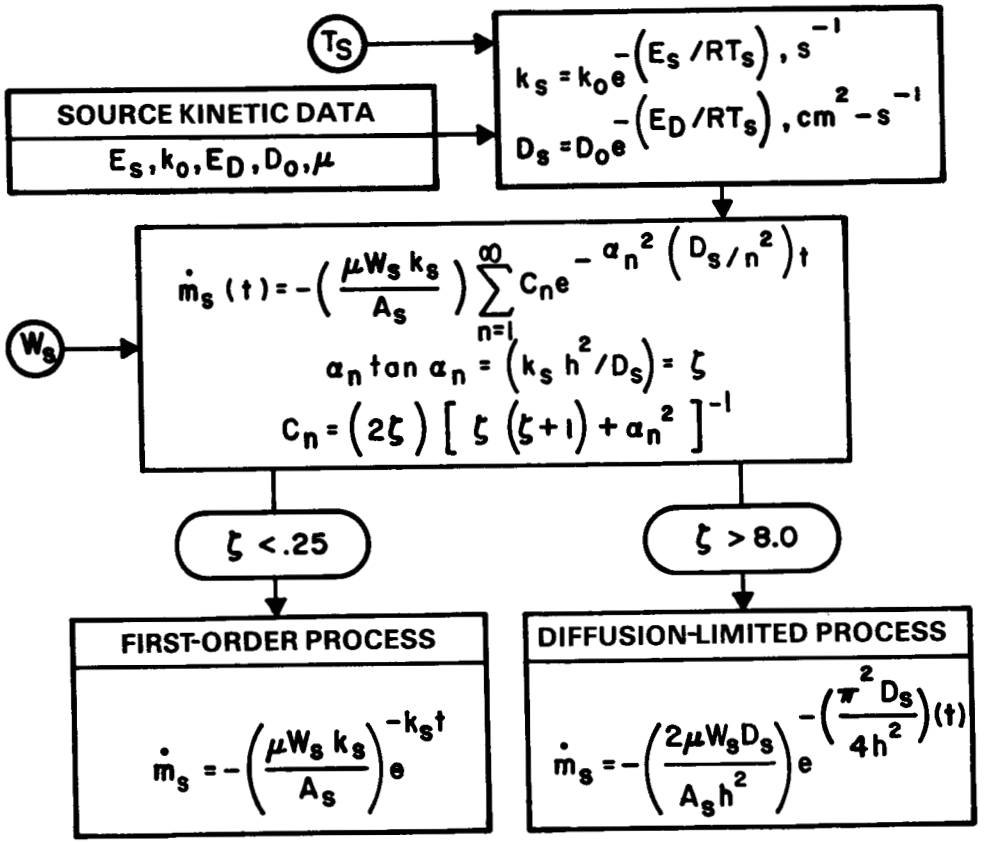

SOURCE VCM EMISSION KINETICS MODEL

FIGURE 1

μ_i = weight fraction of the i^{th} component in the source coating

W_s = total weight of the source coating prior to outgassing, g

A_s = free emission surface of source, cm^2

h = thickness of the source coating, cm.

The source mass loss rate is computed from Fick's First Law[6]

$$\dot{M}_s(t) = A_s \sum_{i=1}^{N} D_i \left[\frac{\partial}{\partial x} C_i(x,t)\right]_{x=0}, \ g\text{-}s^{-1} \tag{3}$$

where

N = number of active components in the source.

It is convenient to define two kinetic parameters for a typical source component.

$$k_{si} = \tau_{si}^{-1} \tag{4a}$$

$$\zeta_i = \left(\frac{h^2 k_{si}}{D_i}\right) \tag{4b}$$

where

τ_{si} = surface residence time for the i^{th} component on the source surface, s

k_{si} = i^{th} component surface rate constant, s^{-1} (also "jump frequency")

h = source coating thickness, cm.

ζ_i is a dimensionless kinetic parameter which specifies the relative importance of surface kinetics to diffusion kinetics for the i^{th} component. A small value of ζ_i indicates that the component has high internal mobility; hence the outgassing is determined primarily by a first-order surface process while a large value of ζ_i indicates a component which is internally diffusion limited.

The complete solution of equation (1) for the total source mass loss rate is given by

$$\dot{M}_s(t) = -W_s \sum_{i=1}^{N} \sum_{n=1}^{\infty} \mu_i \, k_{si} \, C_{ni} \, e^{-\alpha_{ni}^2 D_i t/h^2} \quad g/s \tag{6a}$$

$$\alpha_{ni} \tan(\alpha_{ni}) - \zeta_i = 0 \tag{6b}$$

where

$$C_{ni} = \frac{2\zeta_i}{\zeta_i(\zeta_i+1) + \alpha_{ni}^2}$$

α_{ni} = real and positive rates of the transcendental equation (6b).

When $\zeta_i \leq .1$, all the terms of the infinite series in equation (6a) for $n \geq 2$ are negligible and $\alpha_{1i}^2 \cong \zeta_i$. Equation (6a) then simplifies to a first-order source process.

$$\dot{M}_s(t) = -W_s \sum_{i=1}^{N} \mu_i \, k_{si} \, e^{-k_{si} t}, \; g/s. \tag{7}$$

Exponential kinetics also exists for the general model of equation (6) after sufficient time has elapsed for the exponential terms for $n \geq 2$ in the infinite series to vanish. This "relaxation" time, t^*, is physically the time required for the mass concentration to establish a cosine-like distribution in the source.

The source mass loss rate after the relaxation period is simply the asymptotic solution of equation (6a) when only the fundamental term of the series prevails. The resulting equation is

$$\dot{M}_s(t \geq t^*) = -W_s \sum_{i=1}^{N} \mu_i k_{si} C_{1i} e^{-\alpha_{1i}^2 D_i t/h^2}, \text{ g/s.} \quad (8)$$

For values of $\zeta_i \geq 10$, the fundamental root, α_{1i}, assumes a constant value of $(\pi^2/4)$. This indicates a strongly diffusion-limited process, which can also be simply modeled using exponential kinetics

$$\dot{M}_s(t \geq t^*) \quad -W_s \left(\frac{8}{\pi^2}\right) \sum_{i=1}^{N} \mu_i k_{Di} e^{-k_{Di} t}, \text{ g/s.} \quad (9)$$

where

$$k_{Di} = \left(\frac{\pi^2 D_i}{4h^2}\right), \text{ a diffusion rate constant for the } i^{th} \text{ component, } s^{-1}.$$

The characteristics of outgassing during the transition, or relaxation period, when about 40% of the VCM released must be analyzed by equations somewhat different from (6), since during the initial diffusion process many terms of this series are required. This addition to the source kinetics is currently being prepared. A summary of the surface-mediated diffuse-source kinetics model is shown in Figure 1.

3. VCM Reemission Kinetics

VCM reemission kinetics covers the processes by which condensed VCM desorbs, evaporates, or sublimates from the receptor surface. When sufficient VCM has been deposited on a receptor, the mass reemission rate is constant. If the condensed VCM is a pure substance, this constant reemission rate is dependent upon the saturation vapor pressure through Langmuir equation

$$\dot{M}_L = \frac{A_Q}{\sqrt{2\pi R}} \sqrt{\frac{M}{T_Q}}\, P_\ell \qquad (10)$$

where

$\dot{M}_L$ = Langmuir bulk reemission rate, g/s

M = VCM atomic weight, AMV

T_Q = receptor temperature, °K

P_ℓ = VCM saturation vapor pressure, torr

R = universal gas constant, cal/g-mole-°K.

When the receptor surface is only partially covered, the reemission rate can be related to a temperature-dependent residence time. The rate at which mass leaves a receptor is then the VCM mass deposited on the receptor divided by this residence time. Experiments[7] have shown that a small mass is adsorbed more or less permanently (in vacuum at 10^{-7} torr) on the receptor surface. An equation expressing the VCM reemission rate can then be written

$$M_e(t) = \frac{1}{\tau_e}\left[M_Q(t) - M_a\right] \qquad (11)$$

where

$\dot{M}_e(t)$ = reemission rate, g/s

τ_e = temperature dependent residence time, s^{-1}

$M_Q(t)$ = VCM mass on receptor, g

M_a = VCM permanently adsorbed on receptor, g

The residence time can be shown thermodynamically[8] to have temperature dependence as

$$\tau_e = \tau_o e^{\Delta E_e/RT} \tag{12}$$

where

τ_o = approximately the lattice normal vibrational period, s

ΔE_e = heart of deposition for the process, cal/g-mole

It is easy to see that a first-order reemission rate constant, K_e, similar to that in the source kinetics model, equation (7), can be expressed as the reciprocal of this residence time.

The reemission rate is then essentially a first order process when surface coverage is less than complete.

To account for a continuous process varying from a first-order reemission with small deposits to the constant (zeroth order) mass loss rate limit, when bulk VCM exists, an exponential function is suggested as an initial approximation. The resulting equation bridging equations (1) and (11) becomes

$$\dot{M}_e = -\dot{M}_L \left[i - e^{\frac{k_e}{\dot{M}_L}(M_a - M_Q)} \right] \tag{13}$$

where

$\dot{M}_L$ = Langmuir constant mass loss rate at surface saturation, g/s

$k_e = 1/\tau_e$, reemission rate constant, s^{-1}

The reemission kinetic model is summarized in Figure 2, which illustrates the typical relationships of the parameters at specific receptor temperature. Experimental work has shown that the constant-bulk Langmuir reemission process does not occur until a receptor mass deposit far in excess (>1500 Å thick) of an idealized monolayer coverage exists. The possible explanation for this is that as the VCM leaves the receptor surface, a critical coverage exists where the remaining material tends to draw together and form clusters or islands on the surface. Electron photomicrographs have shown this behavior when the average surface coverage is as much as 500 Å. This is the point where the cohesive surface forces in the VCM exceed the adsorption forces of the VCM to the receptor surface.

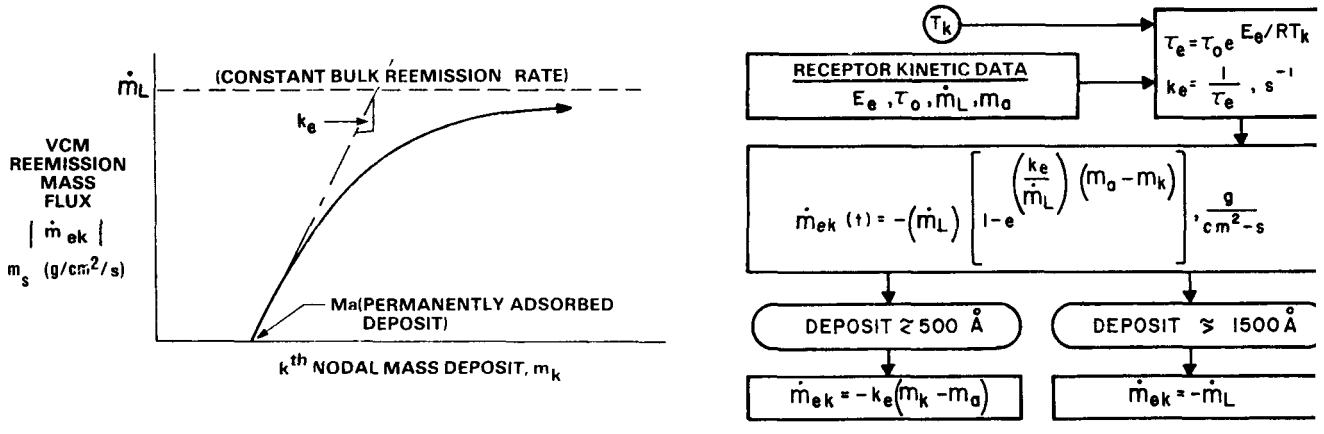

Figure 2. Receptor VCM Reemission Kinetics Model

4. Multinode Transport Model

The transport model mathematically describes the properties of the flow field as the VCM streams between the enclosure nodes. In so doing, it accounts for the intermolecular scattering in the flow field with the boundary conditions ascribed by the source and receptor kinetic models described previously. It is derived in a sequence of three steps. The first is an approximation for the collision integrals in the Boltzmann transport equation which results in a solution of the velocity distribution function (VDF) throughout the flow field. This flow field is statistically modeled by a VDF which relaxes exponentially by repeated binary collisions from its prescribed initial free-molecule value at the nodal surfaces to that of an equilibrium continuum field VDF which is an isotropic background throughout the enclosure. Secondly, the mass flux vector which impinges on each enclosure nodal receptor surface is obtained by integrating VDF over all velocity space (momentum space). The result is the Maxwell integral equation for the first velocity moment. For an N-order multinodal enclosure, this results in a consistent set of N ordinary second-order nonlinear nonhomogeneous differential equations which compute the net mass deposition rate on each node as a function of the source mass loss rate, the nodal reemission rates, and the incident flux of the uniform continuum background. Finally, the mass flux of the continuum field is itself formulated in terms of the source mass loss and nodal reemission rates.

A. The Krook-Boltzmann Relaxation Equation

The starting point for the developing of a statistical analysis for the behavior of gas dynamics is the well known Boltzmann equation. In the absence of external forces on a monatomic homogeneous

gas, this can be written[9]

$$\left(\frac{\partial}{\partial t} + \underline{v}\cdot\nabla\right) f(\underline{r},\underline{v},t) = B(ff') \tag{14}$$

where

$f(\underline{r},\underline{v},t)$ = single-particle velocity distribution function (VDF), molecules/cm^3, at position $\underline{r}$ in space, with thermal velocity $\underline{v}$ at time t.

$B(f,f')$ = bilinear Boltzmann collision integral in functional form.

When the collision probability between two classes (speeds) of molecules is finite, the collision integral can be separated in two parts.[10] One part defines an integral operator for the VDF before scattering, which accounts for the decrease in the VDF due to local removal of molecules, while the second part is a creation collision integral which accounts for molecules added locally to the VDF. The so-called Krook equation[4] expresses this separation by a linearized collision parameter between two VDFs which represent the dynamic state of the gas. This suggests a "relaxation" type process by which each of the VDFs approach each other symmetrically by repeated binary collisions. The Boltzmann collision integral of equation (14) is then approximated by

$$B(ff') \approx -K(f - f_o) \tag{15}$$

where

K = symmetric collision - frequency parameter, s^{-1}

f_o = local Maxwellian VDF

The left side of equation (14) can be interpreted as representing the change in the number of molecules having a VDF of (f) as one follows along a path in phase space through the gas. The Krook simplification proposes that the loss and gain are both proportional to K(i.e., the symmetry of collision), and that the after-collision molecules (f') obey the local continuum Maxwellian VDF. This "two-stream Maxwellian" distribution can be shown[11] to agree with the free-molecule solution at the surface boundaries as well as that of continuum flow regardless of the system geometry. A further simplification assumed for this application is that the continuum field VDF is an absolute Maxwellian, being uniform throughout the enclosure volume but varying in time. This implies the absence of a mass average velocity for this background gas.

Equation (14) combined with (15) can be integrated along a generic direction in physical space which coincides with the velocity vector. The result is a integrable form of the Krook equation

$$\left(\frac{\partial}{\partial t} + v\frac{\partial}{\partial r} + K\right) f\ (r,v,t) = K\ f_o(v,t) \tag{16}$$

This can be readily integrated using the Laplace transform to give the value of the VDF at a remote field point (r_k) from a boundary source point (r_j) in the direction ($\hat{\Omega}$) of the speed (v) as follows.

$$f_k(r,v) = f_j(v,t-r/v)e^{\frac{-K}{v}(r_k-r_j)} + f_o(v,t-r/v)\left[1-e^{\frac{-K}{v}(r_k-r_j)}\right] \tag{17}$$

This is Krook's equation for an enclosure with a spatially isotropic continuum VDF in a direction parallel to the velocity vector. The situation is illustrated in Figure 3.

The translation argument of the time dependent source and field functions indicates that the mass is moving at a finite velocity, hence a time lag of $(r_k - r_j)/v$ is indicated for the field point r_k to be influenced by a flux propagating from source r_j at speed v. If this time lag interval is small compared to the time interval over which the source is changing, then it becomes negligible. This is obviously the case when photons are propagating.

It also applies in the case of satellite structures where the distances between nodes is on the order of tens of meters while molecular velocities are on the order of hundreds of meters per second, since a significant change in the source mass loss rates requires at least several minutes. Thus the final expression for Krook's equation applied to the present systems becomes

$$f_k(r,v,t) = f_j(v,t)e^{\frac{-K}{v}(r_k-r_j)} + f_o(v,t)\left[1-e^{\frac{-K}{v}(r_k-r_j)}\right]. \qquad (17a)$$

B. Enclosure Boundary Conditions

The boundary conditions that need to be specified are the VDF functions at the boundary, f_j, and for the continuum field, f_o. In this simplified model, it is assumed that no average mass velocity develops for continuum flow; hence both VDFs are absolute Maxwellians. The source Maxwellian is assumed to result from a hypothetical equilibrium VCM gas behind the j^{th} source node which results in a cosine distribution of direction relative to the surface normal $(\hat{j})$ with a Maxwellian speed

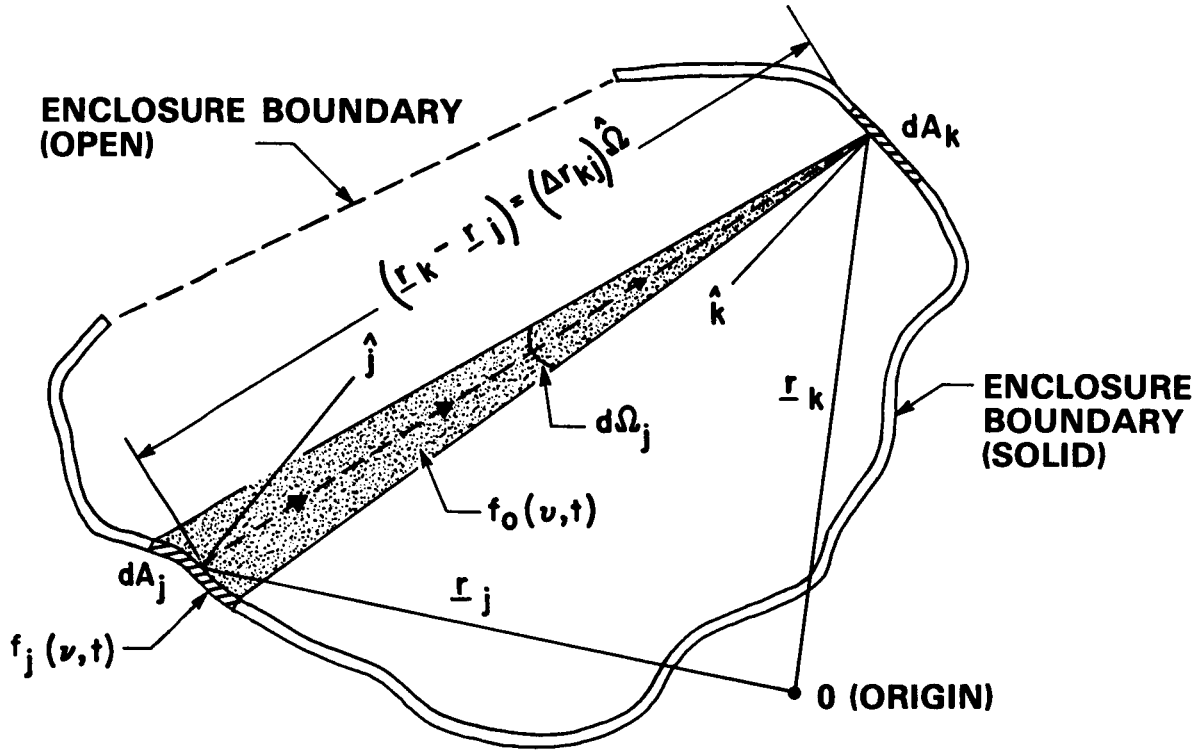

$\underline{r}_j, \underline{r}_k$ = DISPLACEMENT VECTOR TO j^{th} AND k^{th} NODES, cm

$\hat{j}, \hat{k}$ = INWARD SURFACE NORMALS TO j^{th} AND k^{th} NODES

$\hat{\Omega}$ = DIRECTION OF VELOCITY VECTOR, $\underline{V} = |\underline{V}|\,\hat{\Omega}$

f_j, f_o = MAXWELLIAN VELOCITY DISTRIBUTION FUNCTIONS FOR FREE-MOLECULE FLOW AT j^{th} SURFACE AND IN CONTINUUM FLOW FIELD (0), RESPECTIVELY, MOLECULES/cm^3

Figure 3. Enclosure Geometry for Krook Relaxation Model and Mass Intensity

distribution along each radial direction[13]. This further specifies free molecule flow at the surface. Mathematically, this is expressed as

$$f(v,t) = n_j(t)\left(\frac{\beta_j}{\pi}\right)^{3/2} v^2 e^{-\beta_j v^2} \tag{18}$$

where

$n_j(t)$ = molecular number density associated with j^{th} surface node, molecules/cm^3

$\beta_j = \frac{4}{\pi \bar{v}_j^2}$ and

$\bar{v}_j$ = mean thermal speed $= \sqrt{\frac{8kT_j}{\pi m}}$

k = Boltzmann constant, ergs/molecule-°K

m = molecular mass, g/molecule.

In a completely analogous fashion, the continuum field Maxwellian which is independent of spatial orientation can be expressed

$$f_o(v,t) = n_o(t)\left(\frac{\beta_o}{\pi}\right)^{3/2} v^2 e^{-\beta_o v^2} \tag{19}$$

where

$n_o(t)$ = molecule number density for uniform field, molecules/cm^3

$\beta_o = \left(4/\pi\bar{v}_o^{\,2}\right)$.

Since the field Maxwellian is isotropic, it could be integrated along the complete path length to the source node; hence it can be considered directly correlated as if it originated within the surface.

C. Mass Intensity and the Incident Nodal Mass Flux

In fluid mechanics, the principle objective is to determine the macroscopic properties of the flow field such as the average mass velocity, the pressure, shear stresses, and the average energy flow. These average properties, which are functions of the molecular velocity, are calculated at a field point by simply integrating the VDF weighted by the property function over all velocity space. This is formally expressed by

$$\overline{Q}(\underline{r},t) = \int_{\text{All } \underline{v}} Q(\underline{v})\ f(\underline{r},\underline{v},t)\ d\underline{v} \qquad (20)$$

where

$Q(\underline{v})$ = molecular property (mass, momentum, energy)

$d\underline{v}$ = element volume of velocity space.

Another macroscopic average can be obtained for the transport of the property (Q) in a given direction ($\hat{\Omega}$) across an elemental area

normal to that direction. This is obtained by integrating the VDF, now weighted by the property times the projected velocity component, over the hemisphere above the area. The result is called the "property flux vector" and is expressed by

$$\overline{Qv}(r,t) = \int_{\text{half } \underline{v} \text{ space}} Q(\underline{v})\ (\underline{v}\,\hat{\Omega})\ f(\underline{r},\underline{v},t)\ d\underline{v} \tag{21}$$

Thus, the mass flux (vector) is obtained from equation (21) when $Q(\underline{v})$ is designated the molecular mass, and the mass flux is then identified with the first moment of the VDF.

This can be evaluated at the j^{th} source node which will define a "molecular mass intensity," which is analogus to the intensity in radiation heat transfer, for Maxwellian emission from the j^{th} node. The total hemispherical mass loss rate into the enclosure is obtained from the first moment of equation (18).

$$\dot{m}_j(t) = m \int_{(2\pi)} \int_0^\infty v \cos\theta_j\ f_j(v,t)\ dv\ d\Omega \tag{22}$$

where

$\dot{m}_j(t)$ = mass flux leaving j^{th} node, g/cm^2-s

$d\Omega = \sin\theta_j d\theta_j\ d\phi$.

Since the integrals can be separated, the integration over the speeds yields

$$\dot{m}_j(t) = -\int_{(2\pi)} \frac{m}{\pi}\left(\frac{n_j(t)}{2\sqrt{\pi\beta_j}}\right)\cos\theta_j d\Omega, \ g/cm^2\text{-}s. \tag{23}$$

The second integration assumes azimuthal symmetry and ranges θ_j from (0) to ($\pi/2$) thus covering the hemispherical half-space over the j^{th} node. The result is

$$\dot{m}_j(t) = \frac{mn_j(t)}{2\sqrt{\pi\beta_s}} \ , \ g/cm^2\text{-}s. \tag{23a}$$

Recalling the definition of β_j in equation (18),

$$\dot{m}_j(t) = \frac{m\bar{v}_j}{4} n_j(t). \tag{23b}$$

From equation (23) and the definition of uniform intensity, the mass intensity is then defined as

$$I_j(t) = \frac{1}{\pi}\left[\frac{mn_j(t)}{2\sqrt{\pi\beta_j}}\right] = \frac{\dot{m}_j(t)}{\pi} \ g/cm^2\text{-}s\text{-}sr. \tag{24}$$

where

$I_j(t)$ = constant molecular emission intensity from the j^{th} node, g/cm^2-s-sr

An analogous result can be obtained for the intensity of the field mass flux vector since it can be mathematically considered as a source at j^{th} node. The expression becomes

$$I_o(t) = \frac{1}{\pi}\left[\frac{m\, n_o(t)}{2\sqrt{\pi\beta_o}}\right] = \frac{\dot{m}_o(t)}{\pi} \tag{25}$$

where

$I_o(t)$ = constant molecular emission from the field, g/cm^2-s-sr.

$n_o(t)$ = uniform molecular density in the enclosure, g/cm^3.

The differential mass flux on the k^{th} receptor node due to a differential source element dA_j node can be obtained by applying equation (22) with the VDF derived in equation (17). Symbolically, the desired equation becomes

$$d\phi_{j,k}(t) = \int_o^\infty m\, v\, f_k(v,t)\, dv \cos\theta_k\, d\Omega_j \tag{26}$$

where

$\phi_{j,k}(t)$ = mass flux incident on a unit area of the k^{th} node from the j^{th} differential source node, g/cm^2-s.

$d\Omega_j$ = the solid angle subtended at a point in k by the j^{th} node.

If source and field Maxwellians defined by equations (18) and (19) are put into equation (17a) and then the integration indicated in equation (26) is applied, the following expression for the differential mass flux is obtained.

$$d\phi_{j,k} = mn_j \frac{\beta_j}{\pi}^{3/2} \int_o^\infty v^3 e^{-\beta_j v^2 - \frac{k}{v}(r_k - r_j)} dv \cos\theta_k \, d\Omega_j + \text{---}$$

$$\text{--- } + mn_o \left(\frac{\beta_o}{\pi}\right)^{3/2} \int_o^\infty v^3 \left[1 - e^{\frac{-k}{v}(r_k - r_j)}\right] e^{-\beta_o v^2} dv \cos\theta_k \, d\Omega_j . \quad (27)$$

It is convenient to define the following function[11]

$$G_n(\alpha_n) = \frac{1}{2} \int x^3 e^{-x^2 - \gamma_n/x} dx = \langle e^{-\gamma_n/x} \rangle \quad (28)$$

where

$\gamma_n = K\sqrt{\beta_n}(v_j - r_k)$, (n= j,o).

The two integrals of equation (27) can be expressed in terms of function (28),

$$\int_0^\infty v^3 e^{-\beta_j v^2 - \frac{k}{v}(r_k - r_j)} \, dv = \frac{1}{2\beta_j} G_j(r) \tag{29a}$$

$$\int_0^\infty v^3 \left(1 - e^{\frac{-k}{v}(r_k - r_s)}\right) e^{-\beta_o v^2} \, dv = \frac{1}{2\beta_o} \left[1 - G_o(r)\right] . \tag{29b}$$

The solid angle that the j^{th} differential area subtends relative to the k^{th} node is

$$d\Omega_j = \frac{\cos\theta_j \, dA_j}{(r_k - r_j)^2} \tag{30}$$

Now, combining equations (29) and (30) into equation (27) and integrating over a finite source node (A_j) and finite receptor node (A_k), the incident mass flux becomes

$$\phi_{j,k} = \dot{m}_j \frac{1}{A_k} \int_{A_k} \int_{A_j} \frac{G_j(r) \cos\theta_j \cos\theta_k}{\pi (r_k - r_j)^2} \, dA_j \, dA_k + \text{---} \tag{31}$$

$$\text{---} + \dot{m}_o \frac{1}{A_k} \iint \frac{1 - G_o(r) \cos\theta_j \cos\theta_k}{\pi (r_k - r_j)^2} \, dA_j \, dA_k .$$

A mean geometrical molecular transmittance and absorptance can be defined analogous with the characteristics of radiation heat transfer[14] in a scattering and emitting gas as follows

$$(T_{jk}\ F_{jk}) \equiv \frac{1}{A_k}\int_{A_k}\int_{A_j} \frac{G_j(r)\ \cos\theta_j\ \cos\theta_k}{\pi(r_k - r_j)^2}\ dA_j\ dA_k \tag{32a}$$

$$(\alpha_{jk}\ F_{jk}) = \int_{A_k}\int_{A_j} \frac{1 - G_o(r)\ \cos\theta_j\ \cos\theta_k}{\pi(r_k - r_j)^2}\ dA_j\ dA_k \tag{32b}$$

where

T_{jk} = mean geometrical molecular transmittance from the j^{th} to the k^{th} node

α_{jk} = mean geometrical molecular absorptance from the j^{th} to the k^{th} node

F_{jk} = diffuse angle factor from the j^{th} to the k^{th} node

The final form for the mass flux from the j^{th} node incident on the k^{th} node is then finally

$$\phi_{j,k} = (T_{jk}\ F_{jk})\dot{m}_j + (\alpha_{jk}F_{jk})\dot{m}_o. \tag{33}$$

D. Multinode Mass Flux Coupling and Deposition Equations

Equation (33) accounts for the transport of molecular Maxwellian streams between two nodes as indicated. The molecules accounted for by this equation are a composite of two Maxwellian classes, those identified with the source j^{th} node hence at a temperature of T_j and those of the continuum field Maxwellian at temperature T_o. The flux is entirely contained within a volume bounded by the surfaces of the nodes and all straight lines which pass through both nodes. Clearly, this relationship must be extended to include molecules streaming from a node with class temperatures differing from the nodal temperature and should encompass enough nodal surfaces to geometrically describe the system being modeled.

With reference to Figure 4, an "enclosure" is composed of two types of nodes. There are N nodes which form the boundary of the enclosure. These N nodes include open areas, or holes, which are single nodal surfaces which neither scatter (anechoic) or reemit flux. The remainder of the nodes both scatter incident flux and reemit from masses deposited on their surfaces. Each of these "active" nodes is characterized by its area (A_k), its temperature (T_k), by an reemission mass rate ($\dot{m}_{ek}$) at the nodal temperature, and by a group of N capture coefficients (σ_{ik}) which represent the probability that molecules of a Maxwellian class at T_i will reside on the node surface long enough to become accommodated to the nodal temperature, T_r. The fraction of the incident stream that is not accommodated is assumed to be "elastically" scattered; hence it retains its class identification. Both of the emerging streams, the scattered stream at say T_i and the reemitted one at T_k, are assumed to be Maxwellian streams with a cosine

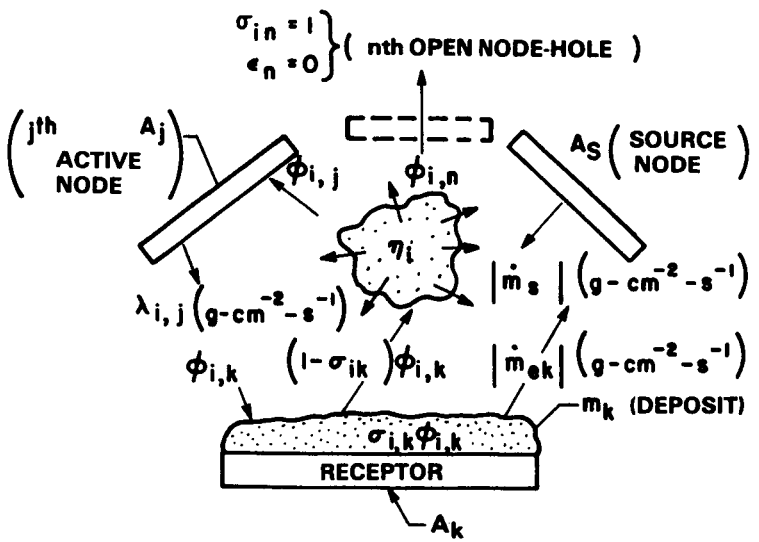

1. INCIDENT MOLECULAR FLUX OF i^{th} CLASS MAXWELLIAN FLUX AT T_i FROM j^{th} NODE TO k^{th} NODE

$$\phi_{i,k} = \sum_{j=1}^{N} \left[\left(T_{ikj} F_{kj} \right) \lambda_{ij} + \left(\alpha_{ikj} F_{kj} \right) \eta_i \right]$$

2. EMERGENT FLUX DUE TO ELASTIC SURFACE SCATTERING AND VCM REEMISSIONS

$$\lambda_{i,k} = \left(1 - \sigma_{ik} \right) \phi_{i,k} + \delta_{ik} \dot{m}_{ek}$$

3. DEPOSITION RATE ON k^{th} RECEPTOR NODE

$$\dot{m}_{dk} = \sum_{i=1}^{N} \left(\sigma_{ik} \phi_{i,k} + \delta_{ik} \dot{m}_{ek} \right) - \sum_{S} \sigma_{sk} F_{ks} \dot{m}_s$$

Figure 4. Enclosure Geometry and Mass Balance Equations

distribution relative to the surface normal.[15] Free-molecule flow is assumed to exist in the immediate vicinity of a nodal surface which becomes "relaxed" within a mean free path of the surface; the so-called Knudsen layer.

The other class of nodes is the source nodes. These are characterized again by their area (A_s), by their temperature (T_s), and by their mass loss rates ($\dot{m}_s$). These nodes may be actually superimposed over one or more of the other nodes or they may be a single-point jet into the enclosure. They do not participate in the scattering and reemission processes. All of the VCM components which are released by the same source are considered as separate VCM sources. In the development of the flux coupling equations which follow, a single VCM component is assumed, to simplify the notation.

With the assumption of each node either totally accommodating and reemitting at its temperature or elastically scattering, it is clear the enclosure VCM gas will be comprised of N Maxwellian classes of molecules. Each of these will be incident and reemitted on each node, resulting in N^2 local mass fluxes. Concomitantly, there will be N continuum field classes which are isotropic throughout the enclosure through which each of the N^2 local surface Maxwellians is relaxing by collision.

The mass flux coupling and mass deposition equations for the enclosure can be derived by considering a VCM mass rate balance on a typical nodal surface, say the k^{th} node, as indicated in Figure 4. The equation for the incident flux of i^{th} class molecules on the k^{th} receptor is obtained by summing over all the enclosure nodes, including the k^{th} node, and over the continuum field fluxes:

$$\phi_{i,k} = \sum_{j=1,N} \left[(T_{ikj} F_{ks}) \lambda_{i,j} + (\alpha_i k_j F_{kj}) \eta_i \right] \qquad (34)$$

$$i,k,j = 1, ---,N$$

where

$\phi_{i,k}$ = total incident mass flux at class temperature T_i on the k^{th} node, g/cm^2-s

$\lambda_{i,j}$ = total mass released from the j^{th} node at temperature T_i, g/cm^2-s (this flux is identical with $\dot{m}_j(t)$ as expressed in previous equations)

η_i = equilibrium field mass flux at T_i (this flux is identical with $\dot{m}_o(t)$ as expressed in previous equations), g/cm^2-s

T_{ikj} = mean transmittance of i^{th} class molecules from the k^{th} node to the j^{th} node

α_{ikj} = mean absorptance of i^{th} class molecules from the k^{th} node to the j_{th} node

F_{kj} = diffuse angle factor from the k^{th} node to the j^{th} node.

In equation (34), use has been made of the reciprocity which is applicable to the scattering process.[14] This is

$$\left.\begin{aligned} A_j\, T_{ijk}\, F_{jk} &= A_k\, T_{ikj}\, F_{kj} \\ \alpha_{ijk} &= (1 - T_{ijk}) \end{aligned}\right\} \qquad (35)$$

The equations for the VCM reemission mass flux can again be identified from Figure 4 and can be expressed as

$$\lambda_{i,k} = (1 - \sigma_{ik})\phi_{i,k} - \delta_{ik}\dot{m}_{ek} \qquad (36)$$

$$i,k = 1,---,N$$

where

σ_{ik} = mean capture coefficient for i^{th} class molecules on the k^{th} node

$\dot{M}_{ek}$ = VCM remission mass flux from the k^{th} node at T_k, (this is intrinsically a negative value, hence the minus sign in equation (36)), g/cm^2-s

$$\delta_{ik} = \begin{cases} 1, & i=k \\ 0, & i\neq k \end{cases} \quad \text{Kronecker delta function}$$

Finally, the nodal mass deposition rates are obtained by summing the accommodated fractions of the incident fluxes with that from the source and subtracting the reemission rate.

$$\dot{m}_{dk} = \sum_{j=1,N} \sigma_{ik}\, \phi_{i,k} + \dot{m}_{ek} - \sigma_{sk}\, T_{sks}\, F_{ks}\, \dot{m}_{s} \qquad (37)$$

where

$\dot{m}_{dk}$ = mass deposition rate for all class molecules on the k^{th} node, g/cm^2-s

$\dot{m}_{s}$ = mass loss rate from the source node at T_s (this is intrinsically a g/cm^2-s negative value, hence the minus sign).

σ_{sk} = mean capture coefficient for s^{th} class source molecules at T_s on the k^{th} node

T_{sks} = mean transmittance for source molecules at T_s from the k^{th} node to the source node

F_{ks} = diffuse view factor from the k^{th} node to the source node.

Now, equations (34) and (36) can be combined to give N^2 linear equations which couple the incident nodal fluxes with the nodal reemission rates and the incident flux from the equilibrium field molecules. This is expressed in matrix format as

$$\left[Y(T_{ikj}\ F_{ks},\ \sigma_{ik})\right]\left\{\phi\right\} = \left[G(T_{ikj}\ F_{kj})\right]\left\{\dot{m}_e\right\} + \left[H(\alpha_{ikj}\ F_{kj}\right]\left\{\eta\right\} \quad (38)$$

where

$\left[Y\right]$ = $(N^2 \times N^2)$ - matrix whose elements are functions of the transmittances, the view factors, and the capture coefficients

$\left\{\phi\right\}$ = (N^2) - vector whose elements are the incident mass fluxes, $g/cm^2\text{-}s$

$\left[G\right]$ = $(N^2 \times N)$ - matrix whose elements are functions of the transmittances and the view factors

$\left\{\dot{m}_e\right\}$ = (N) - vector whose elements are the mass reemission fluxes, $g/cm^{2\text{-}s}$

$\left[H\right]$ = $(N^2 \times N)$ - matrix whose elements are functions of the absorptances and the view factors

$\left\{\eta\right\}$ = (N) - vector whose elements are the incident mass fluxes from the field distribution, $g/cm^2\text{-}s$

Equation (38) can be combined with equation (37), thereby expressing the fundamental mass deposition equations in a concise matrix format:

$$\left\{\dot{m}_d\right\} = \left[I - S(\sigma_{ik})\ Y^{-1}G\right]\left\{\dot{m}_e\right\} + \left[S(\sigma_{ik})\ Y^{-1}H\right]\left\{\eta\right\}\dot{m}_s\left\{B(\sigma_{sk}T_{sks}F_{as})\right\} \quad (39)$$

where

$\left\{ \dot{m}_d \right\}$ = (N) - vector whose elements are the nodal mass deposition rates, g/cm^2-s

$\left[S \right]$ = (N x N^2) - matrix whose elements are the N^2 capture coefficients

$\left\{ B \right\}$ = (N) - vector whose elements are the capture coefficients, the transmittance and the view factors between the receptor nodes and the source

$\left[I \right]$ = (N x N) - identity matrix

When free molecule flow conditions exist through the enclosure, the (α) all vanish and the (T) become unity, and the (H) matrix vanishes. Equation (39) reduces to

$$\left\{ \dot{m}_d \right\} = \left[I - SY^{-1}G \right] \left\{ \dot{m}_e \right\} - \dot{m}_s \left\{ B(\sigma_{sk} F_{ks}) \right\}. \tag{40}$$

At the other end of the collision spectrum the (α) become unity, and the (T) vanish. Further $\left[Y \right] \rightarrow \left[I \right]$, $\left[G \right] \rightarrow 0$, and $\left[H(\alpha F) \right] \longrightarrow \left[H(F) \right]$. Then, the general deposition equation (39) becomes

$$\left\{ \dot{m}_d \right\} = \left[S\ H(F_{kj}) \right] \left\{ \eta \right\} - \left\{ \dot{m}_e \right\}. \tag{41}$$

This shows how the mixing by a very large collision rate (or vanishingly small collision mean free path) substantially homogenizes all of the nodal emission to make up the uniform equilibrium field VCM.

E. Continuum Mass Flux

As shown in equation (39), the nodal deposition rate is linearly dependent on the isotropic continuum flux (η) from the continuum molecules. This continuum, by assumption, is considered to consist of a homogeneous mixture of N vapors with uniform density and N classes of temperatures identified with the nodal temperatures. When continuum conditions exist within the enclosure, all the mass fluxes released from the source and reemitted from the nodes becomes homogenized into the continuum. Since the continuum implies a very large number of intermolecular and surface collisions, it is assumed that the fraction of the total continuum vapor at a particular class temperature will be in the same ratio as the surface area at that temperature to the total bounding area of the enclosure. Thus, each emission and reemission flux regardless of its temperature at release is separated into the N continuum vapors according to this area ratio mixing rule. The incident continuum mass flux is the same on all nodes by virtue of its isotropy.

With these basic properties of the continuum flow field, it is possible to independently derive the continuum nodal mass fluxes in terms of the geometry of the enclosure, the source emission rate, the nodal reemission rate, and the capture coefficients. This is done by performing an instantaneous mass balance within the system enclosure. This simply states the conservation of mass (the continuity equation) of classical continuum fluid mechanics. It is also analogous to the "pumping speed" expression used to evaluate vacuum pumping systems in vacuum chamber technology.[16]

Assuming that continuum flow exists in the enclosure, the rate of change in the total i^{th} continuum class mass in the enclosure is equal to the rate of generation from the source and the nodal reemissions less that adsorbed by capture at the nodal surfaces. Mathematically this is expressed as:

$$\frac{d}{dt}(mN_i) = \left(\frac{A_i}{A_T}\right)\left[A_s \dot{m}_s + \sum_{j=1,N} A_j \dot{m}_{ej}\right] - \frac{1}{4v_o}(mN_i)\, v_i \sum_{j=1,N} A_j \sigma_{ij} \qquad (42)$$

where

N_i = total number if i^{th} class continuum molecules in the enclousre, molecules

A_i = area of the i^{th} node and T_i, cm^2

$A_T = \sum_{j=1,N} A_j$, the total enclosure boundary area, cm^2

v_o = total enclosure volume defined by the envelope of all straight lines passing through two or more nodes, cm^3

$\bar{v}_i = \sqrt{\frac{8kt}{\pi m}}$, the average thermal speed of the i^{th} class of Maxwellian molecules, cm/s

m = molecular mass, g.

The continuum mass flux for the i^{th} class can be expressed as

$$\eta_i = \left(\frac{\bar{v}_i}{4V_o}\right) \cdot mN_i \tag{43}$$

where

η_i = incident mass flux of continuum i^{th} class molecules on all nodes, g/cm^2-s

An ordinary linear nonhomogeneous differential equation for the i^{th} continuum mass flux is then obtained by introducting equation (43) into equation (42) which results in the following expression:

$$\dot{\eta}_i + P_i\eta_i = Q_i \left[A_s\dot{m}_s + \sum A_i\dot{me}_s\right] \tag{44}$$

where

$$P_i = \left(\frac{\bar{v}_i}{4V_o}\right)\sum A_i\sigma_{ij}, \ s^{-1}$$

$$Q_i = \left(\frac{A_i\bar{v}_i}{4V_oA_t}\right), \ cm^{-2}\text{-}s^{-1}$$

For the entire system, the N coupled continuum mass fluxes can be conveniently expressed in matrix format by generalizing equation (44). This set of N equations becomes:

$$\left\{\dot{\eta}\right\} + [P]\left\{\eta\right\} = (A_s\dot{m}_s)[Q] + [Q]\left\{\dot{me}\right\} \tag{45}$$

where

$[\eta]$ = (N) - vector whose elements are the nodal continuum mass fluxes, g/cm^2-s

[P] = (N x N) - diagonal matrix whose elements are the P_i values of equation (44), s^{-1}

[Q] = (N x N) - diagonal matrix whose elements are the q_i values of equation (44), cm^{-2}-s^{-1}

[A] = (N x N) - matrix whose elements are the nodal surface areas, cm^2.

If equation (39) is differentiated with respect to time and equation (45) is substituted in, an ordinary second order differential equation is derived which is linearly dependent upon the continuum flux vector, (η_i). There are then two independent matrix equations which are linearly dependent upon η, equation (30) and its time derivative. If they are combined to eliminate η, a set of N ordinary nonlinear second-order nonhomogeneous differential equations results as follows:

$$[A']\left[\dot{m}_d^{\cdot}\right] + \left\{\dot{m}_d\right\} - [B']\left\{\dot{m}_e^{\cdot}\right\} - [C']\left\{\dot{m}_e\right\} = -\left[\ddot{m}_s\left\{D'\right\} + \dot{m}_s\left\{E'\right\}\right] \quad (46)$$

where

$$[A'] = \left[SY^{-1}\ HP^{-1}\right]\left[SY^{-1}\ H\right]^{-1}$$

$$[B'] = \left[SY^{-1}\ HP^{-1}\right]\left[SY^{-1}\ H\right]^{-1}\left[I\text{-}SY^{-1}\right]G$$

$$[C'] = \left[SY^{-1}\ H\right]\left[P^{-1}AQ\right] + \left[I - SY^{-1}\ G\right]$$

$$\{D'\} = \left(\frac{As}{AT}\right)\left[SY^{-1}\ H\right]\left\{Ai/\sum_j A_i\sigma_{ij}\right\}$$

$$\{E'\} + \{B\} - \left[SY^{-1}\ HP^{-1}\right]\left[SY^{-1}\ H\right]^{-1}\{B\}.$$

Equation (46) is the desired final result of the deposition model. Its format is clarified if first-order reemission kinetics is assured as in equation (11). Assuming that the permanently adsorbed VCM is negligible, the mass rate elements of the deposition equation become:

$$\begin{Bmatrix} m_d \end{Bmatrix} = \begin{Bmatrix} m \end{Bmatrix}$$
$$\begin{Bmatrix} \dot{m}_e \end{Bmatrix} = -[K_e]\, m \tag{47}$$

where

$\begin{Bmatrix} m \end{Bmatrix}$ = (N) - vector whose elements are the specific nodal mass deposit, g/cm^2

When the results of equation (47) are introduced into equation (46), a set of N ordinary second-order nonhomogeneous differential equations for the nodal mass deposition results:

$$[A']\left\{\ddot{m}\right\} + [I + B'K_e]\left\{\dot{m}\right\} + [C'K_e]\left\{m\right\} = -\left[\ddot{m}_s\left\{D'\right\} + \dot{m}_s\left\{E'\right\}\right] \tag{48}$$

which is the deposition equation for very thin deposits.

Equation (48) can be readily solved for the nodal deposition $\left\{m\right\}$ using numerical computation procedures. Since the condition of free molecule flow causes the [H] operator to vanish, the thin-deposit equation (48) simplifies to become:

$$\left\{\dot{m}\right\} + [I - S\ G]\left\{m\right\} = -\dot{m}_s\left\{B\right\} \tag{49}$$

which is equivalent to equation (40). Equation (48) indicates the basic "damping" influence of the continuum flow field. In order to provide

the smooth transition from continuum flow to free molecule flow and vice versa, it is necessary to continually evaluate the changes in the mean geometric transmittances of each node, since these change with the local densities due to the subsequent changes in the collision frequency and the mean free path. Thus, the elements of the matrix operators [Y], [G], [H] and the vector operator $\{B\}$ are functionally dependent on the variable flux vectors $\{\dot{m}_e\}$, $\{\eta\}$, and $\{\phi\}$. This nonlinearity is introduced by the time variations in the magnitude of the fluxes as the source is depleted of VCM. Under free-molecule conditions, when the field is collisionless, the equations becom linear.

Thus, the reduced equation (49) is a significant simplification with constant linear operators and can be solved formally using matrizant methods of matrix calculus together with Sylvestor's theorem for functions of matrices.

A summary of the equations for the multinodal surface contamination model is presented in Figure 5.

● **NODAL SURFACE MASS FLUX EQUATIONS**

$$[\mathcal{Y}(T,F,\sigma)]\{\phi\} = [\mathcal{G}(T,F)]\{\dot{m}_e\} + [\mathcal{H}(1-T,F)]\{\eta\}$$

● **CONTINUUM FIELD MASS FLUX EQUATIONS**

$$\{\dot{\eta}\} + [P(A,\bar{v},V_O,\sigma)]\{\eta\} = [AQ(A,q,\bar{v},V_O)]\{\dot{m}_e\} + A_S\,\dot{m}_S\,[Q]$$

● **NODAL MASS DEPOSITION RATE EQUATIONS**

$$\{\dot{m}_d\} = [\mathcal{S}(\sigma)]\{\phi\} + \{\dot{m}_e\} - \dot{m}_S\{B(T,F,\sigma)\}$$

● **COMBINED MULTINODE DEPOSITION EQUATION**

$$[A']\{\ddot{m}_d\} + \{\dot{m}_d\} - [B']\{\ddot{m}_e\} - [C']\{\dot{m}_e\} = -[\ddot{m}_S\{D'\} + \dot{m}_S\{E'\}]$$

● **DEPOSITION EQUATION FOR FREE-MOLECULE FLOW**

$$\{\dot{m}\} + [I - \mathcal{S}\mathcal{Y}^{-1}\mathcal{G}]\{m\} = -\dot{m}_S\{B\}$$

AEROJET ELECTROSYSTEMS COMPANY

Figure 5. Summary of the Basic Equations of the Multinodal Surface Contamination Model

5. Computational Procedures

To compute the mass deposition on any node with the general conditions of the transitional Knudsen flow, equation (46) must be solved using a digital computer program. The interrelationship of the various equations developed in the previous sections are indicated in the information flow diagram of Figure 6.

Figure 6 depicts three analytical procedures which must be followed prior to exercising the deposition algorithm. These are identified by the double-border rectangles in the upper section of Figure 6. First, the system configuration must be divided into the nodal surfaces which will define the system enclosure. A node is defined as a segment of the enclosure boundary which has a uniform temperature and a uniform mass deposit. The size of a node is dependent only on these two criteria. A system from a small sensor to a large orbiting satellite can be modeled. Once the geometrical characteristics of the enclosure system have been determined, this data is introduced into a geometrical view factor program which is used to compute the diffuse view factors which interconnect the nodes. Many such programs using contour integration and/or finite element integration are available as they are most frequently employed in problems of radiation heat transfer. The third analytical procedure required to support the contamination algorithm is a transient thermal analyzer which can continually compute the nodal and source temperatures over the time period desired. If the system is in a space orbit, the environmental ultraviolet and charged particle fluxes, Φ, should also be computed concurrently with the orbital temperature profiles.

Another very important segment of the overall algorithm is the experimental data base in the four areas indicated on Figure 6 by the circles near the four corners. These test efforts provide the basic

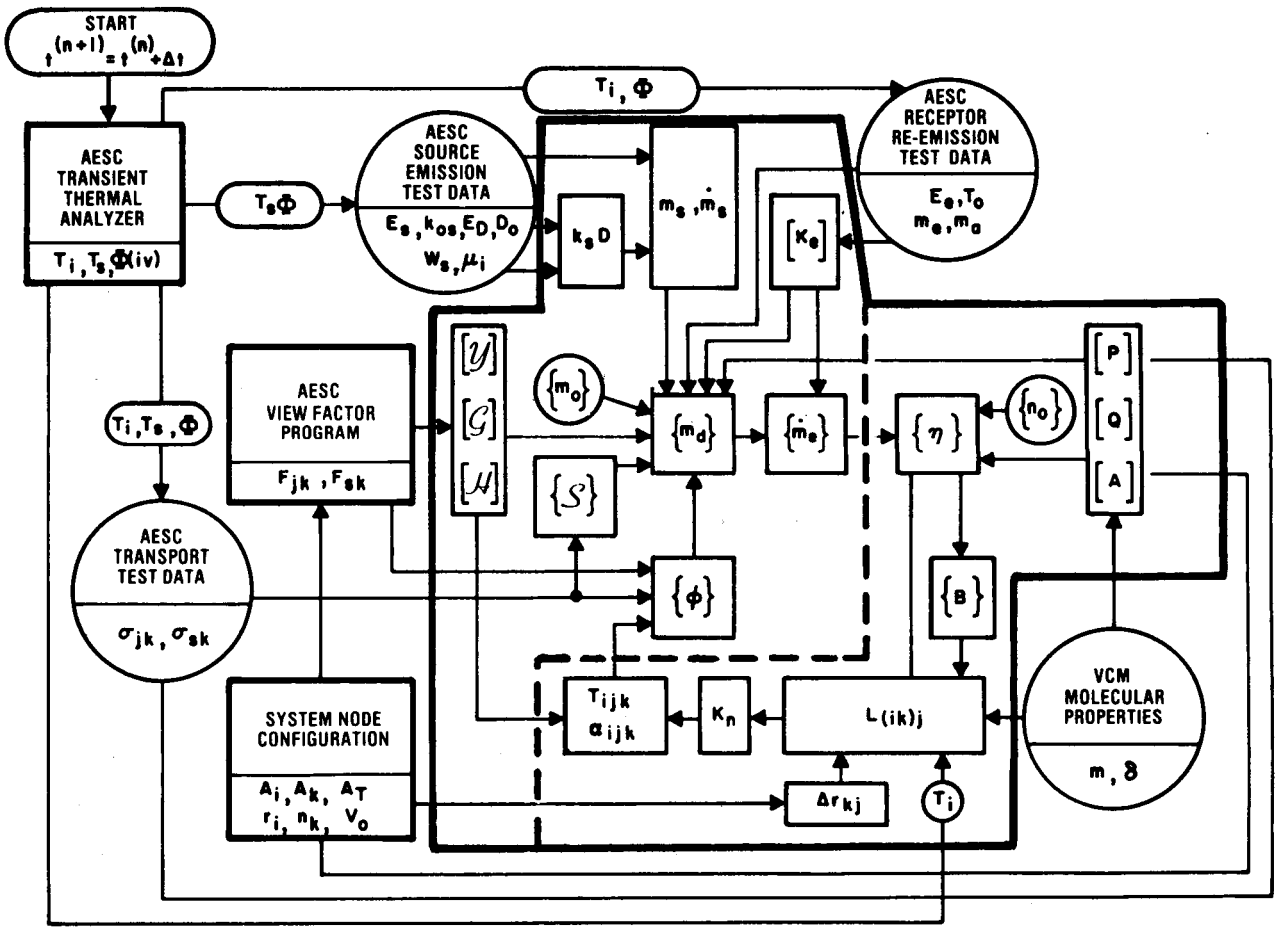

AEROJET ELECTROSYSTEMS COMPANY

Figure 6. Contamination Model Information Flow Diagram

kinetic and transport properties of the sources and their VCM as a function of the temperature of the nodes and of the environmental ultraviolet and particle fluences. Significant progress has been made on obtaining such data for the source emission kinetics, the VCM reemission kinetics, and the capture coefficients which are the transport descriptors for surface collisions.

This data is sufficient if the analysis is to cover only the free-molecule regime. If the scattering influence for transition and continuum flow is necessary, then two VCM molecular properties, the molecular mass (m) and its collision diameter (δ), are needed. For simple monatomic inert gases, fairly good information already exists. However, for the complex polymeric VCM molecules that are released by the source materials used in space, there is virtually no data, and extrapolation from the inert gases is poor at best. Much work is needed in this area.

Another complication enters the computational aspects when transition flow must be considered. This is the problem that the differential equations become nonlinear in that the elements of the operators $[Y]$, $[G]$, $[H]$, and $\{B\}$ become functions of the dependent variables. This requires continual reiteration and computation of the mean free paths and the mean geometric absorptance and transmittance. To use the procedures as indicated on Figure 6, it is implicit that T_{ijk} can be calculated independently of F_{jk}. Generally, as was shown previously, this is not true. However, with relatively simple nonreentrant surfaces, approximate formulas can be used based upon the techniques of radiation heat transfer.[14]

The solution technique is to select an initial orbital time $t^{(o)}$ at which the initial nodal deposit vector is $\{m_o\}$ and the initial continuum flux vector is $\{\eta_o\}$. At the injection of orbit these are both

near zero. The temperatures are then computed. Then, for the time interval, Δt, the temperatures are assumed constant so that the values of the source and receptor kinetic parameters are constant. For this brief period of isothermal conditions, a mass deposition vector is calculated which is then used to determine the scattering mean transmittance for the next Δt interval. Prior to each new Δt, the coefficients of the dependent operators must be recomputed based upon the conditions during the last interval. The informational flow for this loop calculation is outlined in Figure 5 by the dotted boundary. If scattering collisions are negligible, then this block of subprograms is bypassed and the problem solution continues with constant matrix coefficients.

6. Applications

To date, only the free-molecule section of the model has been applied to practical problems. Since only a limited data base presently exists, the results must be considered preliminary, but many of the phenomena attributed to contamination have been at least qualitatively verified on several complex Air Force satellites. Classification of these programs prohibits presentation of the results.

Another relevant application was to use the model to design the apparatus and procedures to measure the kinetic and transport properties of the source materials. It is clear that the nodal coupling is significant and that the configuration of the testing apparatus must be simple enough to permit a closed-form solution of the basic equation (49) in a vacuum chamber. The configuration, sketched in Figure 7, consists of a cylindrical vacuum chamber evacuated to less than 10^{-7} torr with its top, bottom, and sides completely shrouded by LN_2 jacketing. Four quartz crystal microbalances (QCMs)

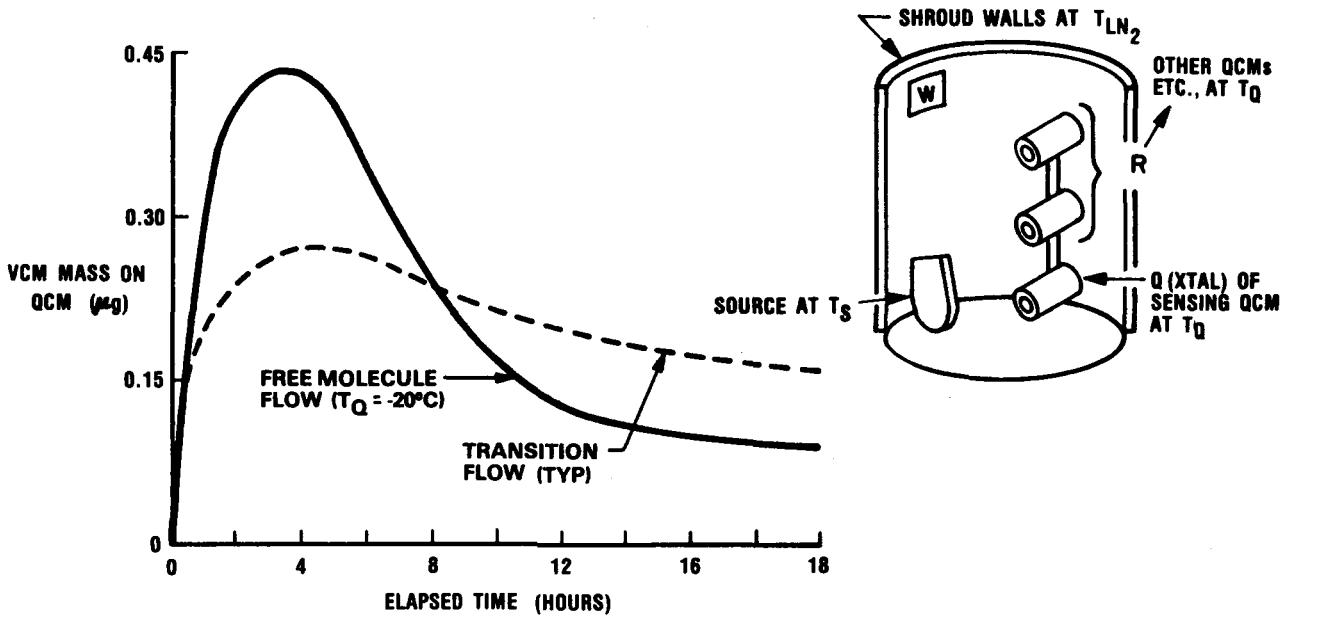

● **DEPOSITION RATE EQUATION**

$$\dot{m}_Q + k_Q m_Q = -F_{QS}\,\sigma_{SQ}\,\dot{m}_S, \text{ g/cm}^2/\text{s}$$

● **MASS DEPOSITION ON INITIALLY CLEAN QCM WITH 1st ORDER SOURCE KINETICS**

$$m_Q(t) = \frac{F_{QS}\,\sigma_{SQ}\,\mu W_S k_S}{A_S (k_Q - k_S)} \left(e^{-k_S t} - e^{-k_Q t}\right), \text{ g/cm}^2$$

Figure 7. VCM Mass (μg) Deposited on a QCM Area 0.316 cm^2 Located 5.0 cm from a 2.54-cm-diameter Source of RTV-566 (0.2% Catalyst) Coated with 70 mg and Maintained at 125°C for 24 Hours.

were positioned at distances varying from 2 inches to 6 inches in front of a 1-inch-diameter disk specimen coated with the source material. The source was maintained at the desired emission temperature between 40°C and 150°C while the QCMs were all collectively held from near LN_2 temperatures (-170°C) to about 25°C. With this configuration the apparatus, labeled the Molekit (Molecular Kinetics Test Facility), can be modeled as a four-node system: the source as a 1-inch-diameter disk, the 1/4-inch-diameter sensing crystal of a particular QCM as another, the remaining QCM cases which can reflect flux, and finally the shroud walls which were assumed to be molecularly anechoic.

When the Molekit is evacuated, free molecular conditions will exist and equation (49), which is linear having constant coefficient matrices, can be solved in closed form for the four-node system. Referring again to Figure 7, let the subscript Q identify the sensing crystal at T_Q, the subscript R identify the other QCMs and the support structure also at T_Q, the subscript S to identify the source held at T_s, and the subscript W to identify the cryoshroud walls at LN_2. The deposition rate on the QCM then becomes:

$$\dot{m}_Q + \sum_j Z_{Qj} m_j = -F_{QS}\sigma_{SQ}\dot{m}_S, \quad (j=Q,R,S,W) \tag{50}$$

where

$$Z_{QQ} = k_Q \left[1-(F_{SW}F_{US} + F_{SQ}F_{QW}F_{US} + \text{---} \right.$$

$$\text{---} + F_{UQ}F_{QS}F_{SW})(1-\sigma_{SQ})(1-\sigma_{QW}) - \ldots$$

$$\left. \ldots -F_{SQ}\,(1-\sigma_{QS}) - F_{WQ}\,F_{QW}(1-\sigma_{QW}) \right]$$

$$\Big/ \left[1 - F_{SW}F_{WS}\,(1-\sigma_{QW})(1-\sigma_{SQ}) \right]$$

$$Z_{QR} = (A_R k_R) \left[(F_{RS}F_{SW}F_{UQ} + F_{RW}F_{WS}F_{SQ})(1 - \sigma_{QS})(1 - \sigma_{QW}) + \right.$$
$$\left. + F_{RS}F_{SQ}(1 - \sigma_{QS}) + F_{RW}F_{WQ}(1 - \sigma_{QW}) \right]$$
$$\frac{}{A_Q \left[1 - F_{SW}F_{WS}(1 - \sigma_{SQ})(1 - \sigma_{QW}) \right]}$$

$$Z_{QS} = -(A_S k_S) \left[F_{SQ} + (F_{SR}F_{RW}F_{WQ} \right.$$
$$\left. - F_{RW}F_{WR}F_{SR})(1 - \sigma_{SQ})(1 - \sigma_{SW}) \right.$$
$$\left. - F_{SW}F_{WQ}(1 - \sigma_{SW}) \right]$$
$$\frac{}{A_Q \left[1 - (F_{RW}F_{WR} + F_{QW}F_{WQ})(1 - \sigma_{SQ})(1 - \sigma_{SW}) \right]}$$

$$Z_{QW} = 0$$

Equation (50) has assumed that all the active nodes are reemitting with first-order processes associated with depositions of less than about 500 Å. The rate constants are k_Q, k_R, and k_S for reemission from the QCM, the support structure, and the source, respectively. k_W, the LN_2 shroud reemission rate constant, is considered to be negligible; hence there is no loss of deposition. However, it is still probable that scattering does occur from the cryogenic shroud walls, hence the presence of the wall capture coefficient, σ_{SW}, in equation (50).

Equation (50) computes the QCM deposition considering all the nodes in a fully coupled system. This is the required model when the spacing between the source disk and the QCM is less than about 1 inch. As this spacing is increased, the view factors diminish rapidly

until, at distances greater than 2 inches, the QCM is coupled only to the source node. With this configuration, equation (50) is dramatically simplified to the intuitively obvious equation

$$\dot{m}_Q + k_Q m_Q = -F_{QS}\sigma_{SQ}\dot{m}_s. \tag{51}$$

If the source mass loss rate, $\dot{m}_s$, can be expressed in an integrable form, equation (51) can be readily integrated. Assuming first-order source kinetics of equation (7) for a source with only one component, the integration of equation (51) using equation (7) for the source, rate assuming an initially clean QCM, gives

$$m_Q(t) = \frac{F_{QS}\sigma_{SQ}W_S k_S}{A_s(k_Q - k_e)}\left(e^{-k_s t} - e^{-k_Q t}\right), \ g/cm^2. \tag{52}$$

Equation (52) shows that the deposition rises to a peak value and then reemits off to zero. The permanently adsorbed layer has been assumed negligible. Figure 7b shows the results of vacuum test data on RTV-566 adhesive compound which represents free molecular conditions. The source was at 125°C while the QCMs and internal support structure were at -20°C. With assumed molecular properties, the "damping" influence of the continuum field can be estimated. A simplified transition model with constant attenuation was used to estimate these effects and compare with free-molecule flow.

The transition flow deposition curve is also shown, with the dotted line, in Figure 7b. The "damping" effect is clear. This is a very real condition when a small cavity surrounds the source as it gasses. For instance, it is highly probable that the total mass loss (% TML) obtained in SRI-JPL tests will be somewhat less than that exhibited in a large vacuum chamber.

References

1. Glassford, A.P.M., "An Analysis of the Accuracy of a Commercial Quartz Crystal Microbalance," paper No. 76-438 presented at the AIAA 11th Thermophysics Conference, San Diego, Cal., 1976

2. "Investigation of Contamination Effects on Thermal Control Materials," AFML-TR-74-218 Final Technical Report, Jan. 1975 (McDonnell Douglas Aerospace Corporation)

3. Buckley, D.H. and Johnson, R.L., "Evaporation Rates for Various Organic Liquid and Solid Lubricants in Vacuum to 10^{-8} Millimeters of Mercury at 55^{o}F to 1100^{o}F," NASA TN D-2081, National Aeronautics and Space Administration, Washington, DC, 1963

4. Bhatnager, Gross, and Krook, in Physical Review (94) pp. 511-525, 1954

5. Lees, L. and Liu, C., "Kinetic Theory Description of Plane Compressible Covette Flow," in Rarefied Gas Dynamics, Supp. 1, 1961

6. Jost, W., Diffusion in Solids, Liquids and Gases, Academic Press, N.Y., 1952

7. Adamson, A.W., Physical Chemistry of Surfaces, John Wiley and Sons, 3rd Ed., 1976

8. Lyubitov, Y., "Molecular Flow in Vessels" in Journal of the Institute of Crystallography, Academy of Sciences of the USSR, Moscow, 1967 (Translation by W. Furrey and J. Wood for the Consultant Bureau, N.Y.)

9. McCune, J.E., Morse, T.F., and Sandri, G., "On the Relaxation of Gases Toward Continuum Flow" in Rarefied Gas Dynamics, p. 115, Supp. 2, Vol. 1, Academic Press, 1963

10. Willis, D.R., "Linearized Covette Flow with Large Knudsen Numbers," in Rarefied Gas Dynamics, p. 429, Supp. 1, Academic Press, 1961

11. Shen, S.F., "A General Transfer Equation Approach for the Transition Regime of Rarefied Gas Flows and Some of its Applications," in Rarefied Gas Dynamics, p. 112, Supp. 2, Vol. II, Academic Press, 1963

12. Patterson, G.N., Molecular Flow of Gases, John Wiley and Sons, N.Y., 1956

13. Nocilla, S., "The Surface Reemission Law in Free-Molecule Flow," in Rarefied Gas Dynamics, p. 327, Supp. 2, Vol. I, 1963

14. Siegel, R. and Howell, J., Thermal Radiation Heat Transfer, McGraw-Hill, 1972

15. Nocilla, S., "On the Interaction Between Stream and Bodies in Free-Molecule Flow," in Rarefied Gas Dynamics, p. 169, Supp. 1, 1961

16. Dushman, S. and Lafferty, J., Scientific Foundations of Vacuum Technique, John Wiley and Sons, Inc., 1962